DOI 10.1007/s10812-023-01530-w
Journal of Applied Spectroscopy, Vol. 90, No. 2, May, 2023 (Russian Original Vol. 90, No. 2, March–April, 2023)

HIGH-SENSITIVITY VIBRATIONAL SPECTROSCOPY USING NANOSTRUCTURES AND ITS APPLICATION TO ART PAINTING RESEARCH

S. V. Gaponenko,[a] E. V. Shabunya-Klyachkovskaya,[b,*] and M. V. Belkov[a]

UDC 535.375.5:75.051

A brief review of surface enhanced Raman scattering (SERS) with metal–dielectric nanostructures and results of its application for cultural heritage studies with paintings as the representative example are presented. Twenty microcrystalline inorganic pigments were successfully detected with 10–100-fold sensitivity enhancement using 1-μg samples.

Keywords: *surface enhanced Raman scattering, plasmonics, photon density of states, cultural heritage.*

Introduction. B. I. Stepanov worked diligently on the formulation of a theory of molecular vibrations in the early stage of his scientific career. The progress of this Leningrad period of his scientific biography was summarized in a well-known monograph [1]. He was recognized together with M. A. El′yashevich and M. V. Vol′kenshtein by a State Award of the USSR. Simultaneously with the development of a theory of molecular vibrations, Stepanov delved into applied issues of vibrational spectroscopy. The present article reviews briefly the achievements in the theory and practice of surface enhanced Raman scattering (SERS) of light due to enhanced interaction of light and a substance in spaces with nontrivial topology characterized by a strong local change of dielectric permittivity of the medium on a scale commensurate with the wavelength of the primary (incident) and secondary (emitted and/or scattered) radiation.

SERS has been observed for organic molecules adsorbed on rough metallic surfaces [2], has been repeated many times using metallic surfaces and nanoparticles (NPs), and has been reduced to the detection of single molecules, which means enhancement of the scattering probability of individual molecules by 10^{10} times and greater [3–10]. Because of the broad use of the term SERS (surface enhanced Raman scattering), we will use the terms SERS-method, SERS-analysis, and SERS-spectroscopy.

The significant increase of Raman scattering (RS) intensity using metallic nanostructures opens possibilities for reducing the cost of equipment required for research by ~10 times, substantially shortening the analysis time, and increasing its sensitivity by many times. Until now, SERS-analysis has not been widely used in practice, despite the relative simplicity of experiments using rough metal surfaces obtained by chemical etching or vacuum deposition and metallic NPs in solutions or deposited onto solid substrates. The reasons for this are as follows. First, the random nature of the metallic surface, the scatter of metallic NP sizes, their frequent uncontrolled aggregation in solutions and upon deposition on substrates, and the effects of various factors on adsorption of analyte molecules on the complex surface hamper metrological calibration and impose a whole series of conditions on sample preparation. Second, SERS-spectra very often differ from RS-spectra of molecules in solutions because of selective enhancement of individual bands, the appearance of enhanced overtones, the appearance of new bands resulting from chemical processes upon adsorption of the analyte onto the metal, and the generation of strong anti-Stokes scattering. The physical reasons for the difference of the secondary radiation spectrum of molecules adsorbed on metal surfaces from their spectra in dilute solutions are the dependence of the excitation intensity on the polarization direction of the incident radiation for different vibrational modes of adsorbed molecules, the dependence of the density of photon states on the frequency of the secondary radiation, and the nonlinearity of vibrations of highly excited

*To whom correspondence should be addressed.

[a]B. I. Stepanov Institute of Physics, National Academy of Sciences of Belarus, Minsk, Belarus; [b]Yanka Kupala Grodno State University, Grodno, Belarus; email: elena.shabunya@gmail.com. Translated from Zhurnal Prikladnoi Spektroskopii, Vol. 90, No. 2, pp. 156–164, March–April, 2023. Original article submitted February 10, 2023; https://doi.org/10.47612/0514-7506-2023-90-2-156-164.

molecules. Third, enhancement of RS often occurs simultaneously for all molecules in the solution being analyzed, which does not allow the detection sensitivity of certain molecules to be increased in actual experiments but simply shortens the RS signal accumulation time or allows less sensitive equipment to be used for the measurements. This problem can be solved by development of specific methods for each analytical task based on selective detection of the target molecules by adding to the solution or mixture additional molecules that interact chemically with the target molecules. Then, the task of detection reduces to the observation of new specific bands in the analyte vibrational spectrum that indicate the formation of bonds of the additionally added molecules with the molecules slated for detection. Examples of such an approach are experiments of scientists at the B. I. Stepanov Institute of Physics, NAS of Belarus, on the detection of antimony [11] and bromate ions in drinking water [12].

As a minimum for two areas of analytical spectroscopy tasks, i.e., criminalistics and research on cultural heritage items, the primary task is not quantitative analysis of the molecular composition of complex mixtures but qualitative analysis to identify compounds present in mixtures. Namely this last area is the subject of the present work.

SERS theory. The theory of SERS from the observation of SERS in 1974 to the end of the last century consisted mainly of calculations of the electromagnetic radiation strength E for model metallic structures as a function of incident radiation frequency ω_0. The function $E(\omega_0)$ increases by 2–3 orders of magnitude at certain so-called hot points on metallic nanostructures, e.g., in gaps between two and more closely positioned NPs. It was assumed that the field strength for secondary radiation with frequency ω was enhanced in an analogous manner. It was also supposed that the similarity of frequencies ω_0 and ω allowed the increase in the strength of the primary and secondary radiation to be considered equal, i.e., $E(\omega_0)/E(\omega) = E(\omega)/E(\omega_0)$. As a result, the increase in the probability of RS was taken as proportional to $[E(\omega)]^4$, with E_0, the electric field strength in free isotropic space with dielectric constant $\varepsilon = 1$. The theoretical studies of this period have been reviewed [13]. It was shown in 2002 [14, 15] that photon scattering, like their spontaneous emission, should have a probability proportional to the density of photon states (electromagnetic modes). The change in the probability of spontaneous transitions in media different from a vacuum because of a change in the density of photon states was well known by that time and was called the Purcell effect after the author of the pioneering work [16]. The development of concepts about the effect of the density of photon states on optical processes from the pioneering work of S. N. Bose (1924) to the present was described before [17]. The correlation of the probability of photon scattering and the density of photon states was experimentally established for waveguides, photonic crystals, and cavities [18–20]. In general, the change of RS probability F_{scatt} at frequency ω by a molecule (or nanocrystal or small atomic cluster) located at point $\mathbf{r}$ near a metallic nanosized object and excited by radiation with frequency ω_0 can be written

$$F_{\text{scatt}} = \frac{I(\mathbf{r}, \omega)}{I_0(\mathbf{r}, \omega)} = \frac{\left|\boldsymbol{E}(\mathbf{r}, \omega_0)\right|^2}{\left|\boldsymbol{E}_0(\mathbf{r}, \omega_0)\right|^2} \frac{D(\mathbf{r}, \omega)}{D_0(\omega)} = \frac{\left|\boldsymbol{E}(\mathbf{r}, \omega_0)\right|^2}{\left|\boldsymbol{E}_0(\mathbf{r}, \omega_0)\right|^2} \frac{\gamma_{\text{rad}}(\mathbf{r}, \omega)}{\gamma_0(\omega)}, \quad (1)$$

where I and I_0 are the intensities of the secondary radiation near the nanosized object and in a vacuum; $D_0(\omega) = \omega 2/\pi^2 c^3$, the density of photon states in a vacuum (c, speed of light in a vacuum); $D(\mathbf{r}, \omega)$, density of photon states at point $\mathbf{r}$; γ_{rad}, rate of spontaneous radiative transitions changed by the presence of the nanosized object; γ_0, rate of spontaneous radiative transitions in a vacuum. According to Eq. (1), the intensity of scattering and spontaneous emission of photons near the nanosized object vary in the same manner on the condition that the presence of the nanosized object does not change the photoluminescence (PL) quantum yield. Thus, on one hand, the change in the probability of spontaneous transitions can be predicted from the measured scattering spectra and, on the other, the change of photon scattering probability can be predicted from the calculated probability of spontaneous transitions. This refers to both RS and resonant Rayleigh scattering of light. The latter is simpler to measure experimentally as a nondissipative component in the extinction spectrum of metal–dielectric nanostructures. This property of complex nanostructures to affect identically various types of secondary radiation was discussed in detail [21] and was confirmed experimentally [22].

Thus, the theory of SERS near a nanosized object, including metallic NPs and surfaces with complicated topology, reduces to a calculation of the incident radiation intensity at the point where the scattering object is located and the density of photon states at the same point at the frequency of the secondary radiation. The density of photon states can be found from the calculated change in the rate of spontaneous transitions $\gamma_{\text{rad}}/\gamma_0$. The value of $\gamma_{\text{rad}}/\gamma_0$ can be calculated from the solution of problem of a classical emitter near a nanosized object. This approach to calculating $\gamma_{\text{rad}}/\gamma_0$ was proposed before [23]. It allows the problem of photon emission by a quantum system to be treated as a problem of the emission of radiation by a classical oscillator, obeying the unique correspondence principle (transition from radiophysics to quantum electrodynamics)

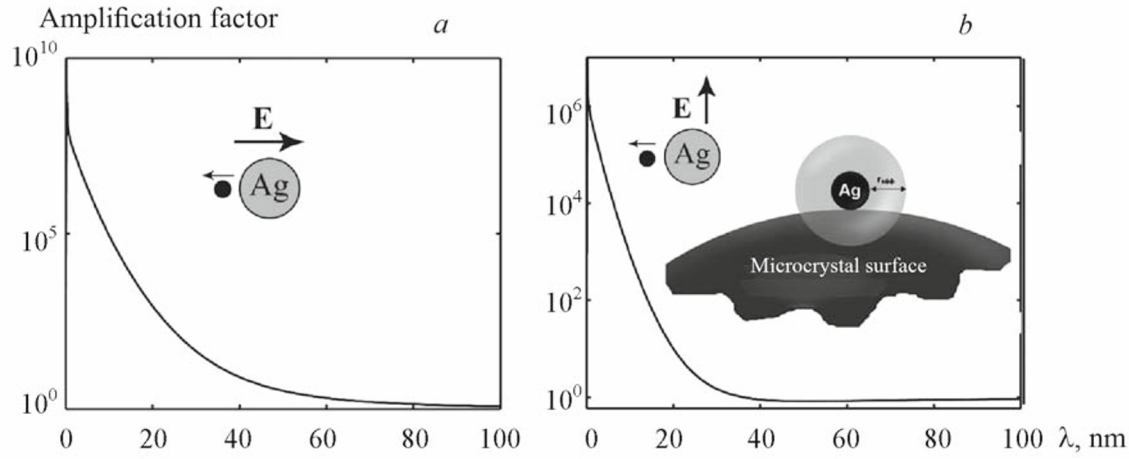

Fig. 1. Increased probability of RS calculated using Eqs. (1)–(3) as a function of distance from a metal surface to a molecule for vibrations of frequency 10^3 cm^{-3} (λ_{ex} = 532 nm, Ag NP diameter 20 nm) and tangential (a) and normal polarization (b) of incident radiation; the molecular dipole moment is oriented as shown by the arrow and selected normal to the metallic particle surface to obtain the maximum SERS enhancement factor; in the inset, explanation of the possibility of producing SERS for large microcrystals.

in agreement with the operational definition of local density of photon states [24] and the subsequent development of the optical antenna concept [25]. It is noteworthy that the concept of an optical antenna, like that of controlling RS using a space with a complicated topology, is broader than the SERS problem and includes not only metallic and metal-dielectric but also purely dielectric nanostructures [26, 27]. Equation (1) for several model problems (single spherical particle or dimer of two such particles, an ellipsoid) can be calculated analytically, as demonstrated for enhanced luminescence [27, 28], and then used for analysis in SERS-spectroscopy [29–32]. For example, the intensity for normal and tangential polarization of incident radiation for a single spherical NP of radius $a << 2\pi c/\omega$ in a vacuum (or in air) is:

$$\frac{\left|\mathbf{E}(\mathbf{r},\,\omega_0)\right|^2}{\left|\mathbf{E}_0(\mathbf{r},\,\omega_0)\right|^2} = \left|1 + \sigma\left(\frac{\varepsilon(\omega_0) - 1}{\varepsilon(\omega_0) + 2}\right)\left(\frac{a}{r}\right)^3\right|^2, \tag{2}$$

where $\sigma = +2$ for normal and $\sigma = -1$ for tangential polarization of the incident radiation [28, 33]. The change in the rate of spontaneous transitions and the density of photon states for a spherical particle, in full agreement with the concept of an optical antenna, is described by the analogous equation

$$\frac{D(\mathbf{r},\,\omega)}{D_0(\omega)} = \left|1 + \sigma\left(\frac{\varepsilon(\omega) - 1}{\varepsilon(\omega) + 2}\right)\left(\frac{a}{r}\right)^3\right|^2, \tag{3}$$

although here normal and tangential orientation is understood to refer to the molecular dipole moment and the dielectric permittivity is examined at the frequency of the secondary radiation.

Figure 1 shows an example of a calculation using Eqs. (2) and (3) for Ag NPs [31]. The enhancement factor is observed to be $>10^7$ even for a single NP for the optimal orientation of the molecular dipole moment and polarization of incident radiation. However, the enhancement quickly drops with distance and is practically absent at distances >50 nm from the metal NP.

Introduction of the local density of photon states into the SERS theory explains not only the enhancement factors for various vibrational modes but also the selective enhancement of the anti-Stokes components in the SERS [34] that is observed experimentally. The latter allowed laser cooling of molecules using enhanced anti-Stokes SERS to be proposed [35].

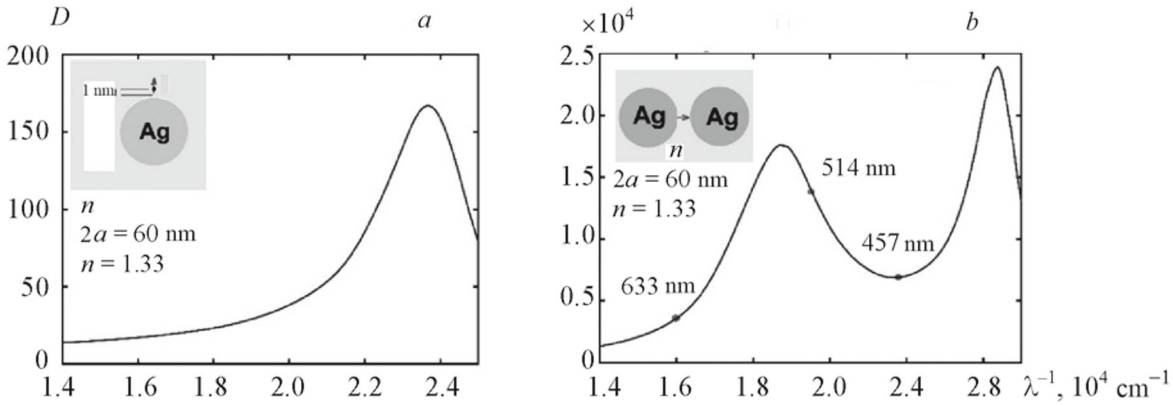

Fig. 2. Local density of photon states as a function of wavenumber at 1 nm from Ag NP of diameter 660 nm (a) and between two NPs (b) for normal orientation of dipole moment of probe molecule located in aqueous solution (n = 1.33) [34]; typical wavelengths of commercial lasers (633, 514, and 457 nm) used in systems for studying RS are indicated.

Figure 2 shows calculated densities of photon states as functions of wavenumber λ^{-1} (secondary radiation) for a single Ag NP and a dimer of two NPs. The enhancement factor of the incident radiation intensity changes analogously, which allows a total increase of RS intensity of ~10^{10} to be obtained on going from a single NP to the dimer. It is noteworthy that the spectral dependence of the density of states gives various scattering enhancement factors for various modes and is the primary physical reason for the difference of the SERS spectra from the standard RS spectra.

Application of SERS-Spectroscopy to the Study and Attribution of Paintings. Easel paintings with up to 10 and more different components forming a complicated multi-component multi-layered structure are among the most complicated paintings to analyze. A binding intermediate layer, ground coating, imprimatura, drawing (in several instances), paint layers themselves, and protective layer are successively applied from the base to the surface [36]. The whole available arsenal of nondestructive physicochemical methods, including x-ray studies to obtain information about the number and general structure of the layers, atomic emission analysis, optical microscopy, x-ray phase analysis to identify crystalline inclusions, and molecular analysis by vibrational spectroscopy (Raman and IR spectroscopy) should be enlisted for a comprehensive analysis of such a complicated object. A comprehensive attribution can be made only by including additional information about the origin of a picture and pigments and auxiliary components typical of various historical periods and art schools.

RS spectroscopy is rather widely used to study cultural heritage objects, including paintings [37, 38]. SERS-spectroscopy is also used in such studies to identify organic components in paintings [39–41]. An example of the successful use of SERS-spectroscopy to identify organic pigments in paintings could be the result for malachite green (Fig. 3). Elongated Au NPs (nanorods) were used to increase the RS signal level by a minimum of an order of magnitude. The pigment could be identified by analyzing a sample of ~1 μg using standard equipment for recording RS and SERS. A significant part of art pigments consists of inorganic compounds as crystallites of sizes from hundreds of nanometers to 10 μm. The use of inorganic pigments is explained primarily by their high photochemical stability as compared to organic pigments and the availability in minerals. The crystallite sizes in such pigments are determined, on one hand, by the ability to prepare them by grinding and, on the other, the light-scattering conditions. SERS was investigated only for organic molecules before the start of the 21st century for about three decades. It is important that the typical size of the molecules was several nanometers, i.e., an order of magnitude smaller than typical NPs or the heterogeneity in metal–dielectric nanostructures. A systematic investigation of SERS-spectroscopy for semiconducting nanocrystals, the size of which was commensurate with molecular dimensions and much less than the size of metallic nanosized objects used to enhance secondary radiation, began only in 2009 [42–45]. SERS for ZnO nanocrystals allowed them to be proposed as a nonresonant narrow-band label for detection of biomolecules instead of the traditionally used broadband fluorescent labels that require a certain excitation wavelength [45]. A regular question arising during this period was whether SERS-spectroscopy could be expanded to large crystallites. We postulated and successfully performed experiments first for model and laboratory and then for actual art samples of microcrystalline pigments to answer it. The first experiments demonstrated enhancement by 1–2 orders of magnitude of RS signals from ultramarine microcrystals for nanotextured Si–Ge substrates coated with gold and silver (Fig. 4) [46, 47]. The

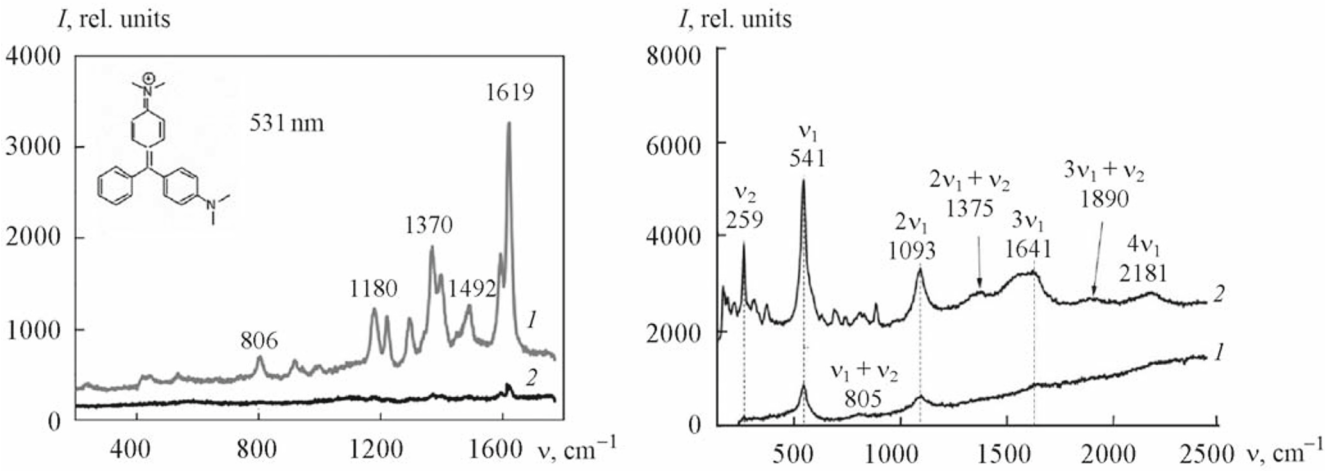

Fig. 3. Enhanced (1) and ordinary RS (2) for malachite green pigment obtained using Au nanorods.

Fig. 4. RS spectrum of microcrystalline ultramarine *in vitro* (in a capillary) (1) and SERS spectrum using metallized nanotextured Si–Ge substrate (2).

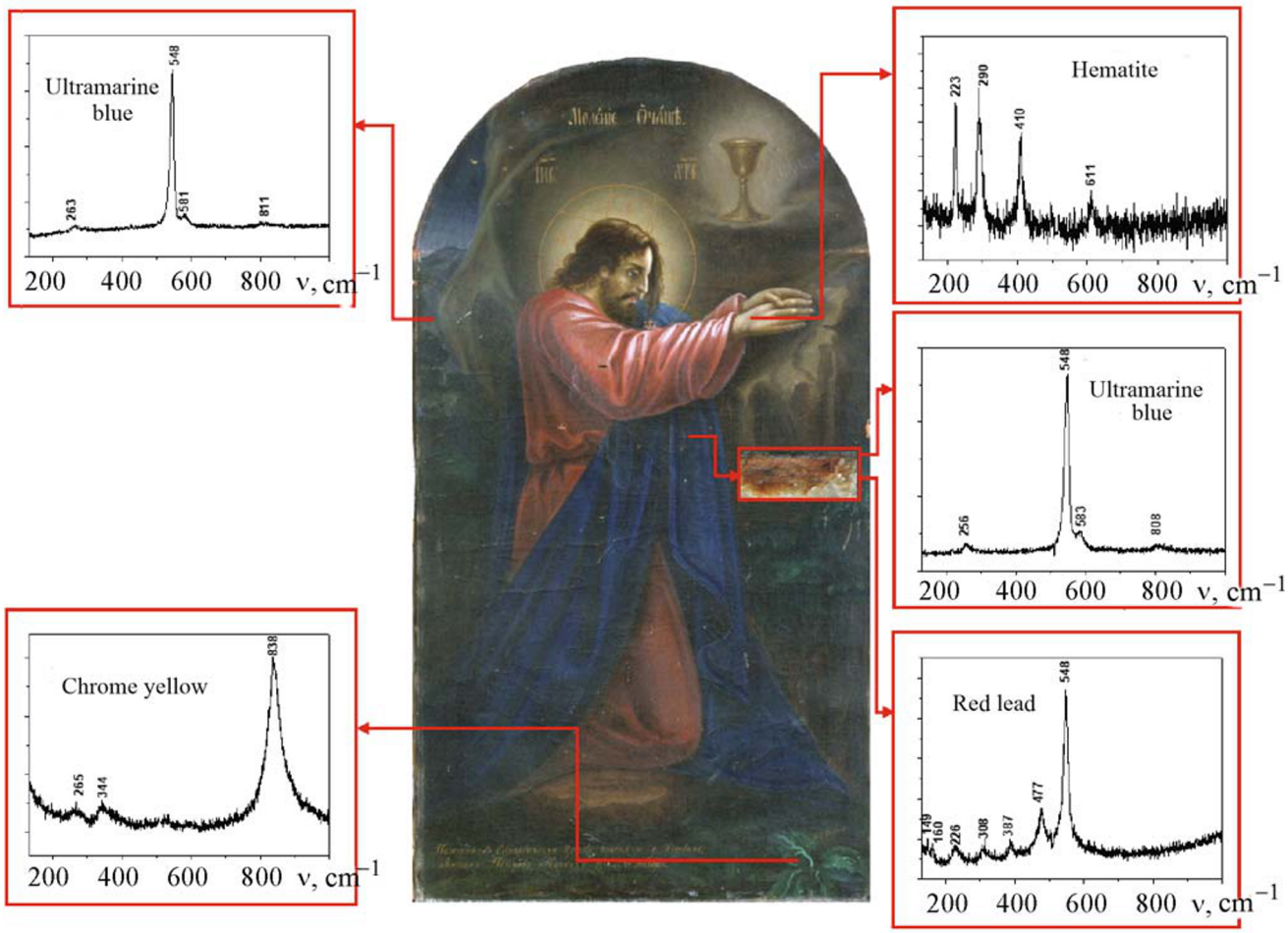

Fig. 5. Detection by SERS of inorganic pigments in icon of Zh. E. Shorokhov *Agony in the Garden* (1882) from Zhirovichi (Synkovichi), Slonimskii District, Grodno Region (from the collection of the Ancient Belarusian Culture Museum, National Academy of Sciences of Belarus).

TABLE 1. SERS Spectroscopy of Inorganic Microcrystals in Paintings

Pigment	Wavelengths, nm	Nanostructures	Reference
Anatase (TiO_2)	488	Au	[50, 51]
Azurite [$2CuCO_3 \cdot Cu(OH)_2$]	488, 531	Au	[49–51]
Cadmium yellow (CdS)	488	Au	[50, 51, 53]
Azure ($CoO \cdot nSnO_2$)	488, 531	Au, Ag	[50, 51, 53]
Chalk ($CaCO_3$)	488	Au	[50, 52]
Chrome green (Cr_2O_3)	488	Au	[50]
Chrome yellow ($PbCrO_4$)	488	Au	[50]
Cinnabar (HgS)	632.8	Ag/Si/Ge Au/Si/Ge	[48, 50]
Cobalt titanate green (Co_2TiO_4)	531	Au, Ag	[51]
Glauconite $\{K[(Al^{III},Fe^{III})(Fe^{II},Mg^{II})],(AlSi_3,Si_4)O_{10}(OH)_2\}$	488	Au	[51]
Malachite [$CuCO_3 \cdot Cu(OH)_2$]	531	Au, Ag	[51]
Lead oxide (PbO)	488	Au	[50, 51]
Praseodymium yellow [$(Zr,Pr)SiO_4$]	531	Au, Ag	[51]
Rutile (TiO_2)	488	Au	[51, 53]
Ultramarine blue [$Na_8(Al_6Si_6O_{24})Sn$]	488, 531	Au, Ag Au/Si/Ge Ag/Si/Ge	[32, 46, 47, 49]
Ultramarine violet [$Na_8(Al_6Si_6O_{24})Sn$]	531	Au, Ag	[51]
Viridian $Cr_2O_3 \cdot H_2O$	531	Au, Ag	[51]
Zinc white (ZnO)	531	Au, Ag	[51]
Hematite (Fe_2O_3)	531	Al	This work
Red lead (Pb_3O_4)	531	Al	This work

ultramarine RS-spectrum was not recorded on the background noise for an uncoated metal substrate; except for overtones and combination modes that were revealed by multiple ($>10^2$ times) enhancement of the signal. Later, SERS experiments were performed for another 19 microcrystalline inorganic pigments used in painting (Table 1) [46–53]. An overall database of their SERS-spectra was compiled [51]. In all instances, the RS signal was relatively easily enhanced up to10 times and up to 100 times in several instances. An interpretation of the results proposed that a microcrystal several micrometers in size was surrounded by NPs 20–60 nm in size, each of which (according to Figs. 1 and 2), enhanced RS in the subsurface region with quenching in the bulk. As a result, the significant SERS effect persisted to crystallite sizes of several microns. The RS signal could be additionally enhanced by using a sandwich configuration in which a thin layer of the analyte was situated between two layers of metallic NPs [53].

Figure 5 shows an example of the use of SERS-spectroscopy for an actual painting from the collection of the Ancient Belarusian Culture Museum, NAS of Belarus. Figure 5 demonstrates the identification of four inorganic pigments, for two of which (red lead and hematite) SERS-analysis was applied for the first time. Understandably, SERS is not the only possible method for spectral analysis of cultural heritage objects. It is supplemented by atomic spectral analysis, e.g., using a portable dual-pulse laser spectrometer developed at B. I. Stepanov Institute of Physics, NAS of Belarus, for a comprehensive investigation [54–56].

Conclusions. Introduction of a modified local density of photon states at the frequency of secondary radiation into the theory of SERS by metallic NPs enabled this phenomenon to be correctly described and made it possible to calculate the probability and scattering intensity by analogy with the probability of spontaneous transitions and photoluminescence intensity. Correct consideration of the modified local density of photon states explained the enhancement factors for various vibrational modes and excitation wavelengths of emission, including anti-Stokes anomalies known in the practice of SERS-spectroscopy. It was shown based on studies of 20 various pigments that SERS-spectroscopy could be used effectively to identify inorganic crystalline art pigments and could be used with samples from 1 μg.

Acknowledgment. The work was dedicated to the 110th birthday of Acad. B. I. Stepanov, one of the founders of the Belarusian Optics School, which contributed greatly to the development of vibrational spectroscopy in Belarus.

REFERENCES

1. M. V. Vol′kenshtein, M. A. El′yashevich, and B. I. Stepanov, *Molecular Vibrations* [in Russian], GITTL (1949).
2. M. Fleischmann, P. J. Hendra, and A. J. McQuilaan, *Chem. Phys. Lett.*, **26**, 163–166 (1974).
3. K. Kneipp, H. Kneipp, I. Itzkan, R. R. Dasari, and M. S. Feld, *Chem. Rev.*, **99**, 2957–2976 (1999).
4. B. Sharma, R. R. Frontiera, A. I. Henry, E. Ringe, and R. P. Van Duyne, *Mater. Today*, **15**, 16–25 (2012).
5. N. Strekal, A. Maskevich, S. Maskevich, J. C. Jardillier, and I. Nabiev, *Biopolymers*, **57**, 325–328 (2000).
6. A. M. Michaels, J. Jiang, and L. Brus, *J. Phys. Chem. B*, **104**, 11965–11971 (2000).
7. P. A. Mosier-Boss, *Nanomaterials*, **7**, 142–171 (2017).
8. J. Langer, D. Jimenez de Aberasturi, J. Aizpurua, R. A. Alvarez-Puebla, B. Auguie, J. J. Baumberg, G. C. Bazan, S. E. Bell, A. Boisen, A. G. Brolo, and J. Choo, *ACS Nano*, **14**, 28–117 (2019).
9. A. K. Sarychev, A. Sukhanova, A. V. Ivanov, I. V. Bykov, N. V. Bakholdin, D. V. Vasina, V. A. Gushchin, A. P. Tkachuk, G. Nifontova, P. S. Samokhvalov, A. Karaulov, and I. Nabiev, *Biosensors*, **12**, 300–310 (2022).
10. Y. Liu, Y. Zhang, M. Tardivel, M. Lequeux, X. Chen, W. Liu, J. Huang, H. Tian, Q. Liu, G. Huang, and R. Gillibert, *Plasmonics*, **15**, 743–752 (2020).
11. A. Y. Panarin, I. A. Khodasevich, O. L. Gladkova, and S. N. Terekhov, *Appl. Spectrosc.*, **68**, 297–306 (2014).
12. O. S. Kulakovich, E. V. Shabunya-Klyachkovskaya, A. S. Matsukovich, K. Rasool, K. A. Mahmoud, and S. V. Gaponenko, *Opt. Exp.*, **24**, A174–A179 (2016).
13. K. Kneipp, M. Moskovits, and H. Kneipp (eds.), *Surface-Enhanced Raman Scattering: Physics and Applications*, Springer Science & Business Media (2006).
14. S. V. Gaponenko, *Phys. Rev. B: Condens. Matter Mater. Phys.*, **65**, Article ID 140303 (2002).
15. V. S. Zuev and A. V. Frantsesson, *Opt. Spectrosc.*, **93**, 108–117 (2002).
16. E. M. Purcell, *Phys. Rev.*, **69**, 681–681 (1946).
17. S. V. Gaponenko, *J. Nanophotonics*, **8**, Article ID 087599 (2014).
18. S. Guddala, S. A. Kamanoor, A. Chiappini, M. Ferrari, and N.R. Desai, *J. Appl. Phys.*, **112**, Article ID 084303 (2012).
19. K. Inoue, H. Oda, A. Yamanaka, N. Ikeda, H. Kawashima, Y. Sugimoto, and K. Asakawa, *Phys. Rev. A: At., Mol., Opt. Phys.*, **78**, 011805 (2008).
20. H. Sumikura, E. Kuramochi, H. Taniyama, and M. Notomi, *Appl. Phys. Lett.*, **102**, Article ID 231110 (2013).
21. S. V. Gaponenko and D. V. Guzatov, *Proc. IEEE*, **108**, 704–720 (2020).
22. Y. Chen, K. Munechika, I. Jen-La Plante, A. M. Munro, S. E. Skrabalak, Y. Xia, and D. S. Ginger, *Appl. Phys. Lett.*, **93**, Article ID 053106 (2008).
23. V. V. Klimov, M. Ducloy, and V. S. Letokhov, *Euro. Phys. J. D*, **20**, 133–148 (2002).
24. G. D'Aguanno, N. Mattiucci, M. Centini, M. Scalora, and M. J. Bloemer, *Phys. Rev. E: Stat., Nonlinear, Soft Matter Phys.*, **69**, Article ID 057601 (2004).
25. P. Bharadwaj, B. Deutsch, and L. Novotny, *Adv. Opt. Photonics*, **1**, 438–483 (2009).
26. A. E. Krasnok, A. E. Miroshnichenko, P. A. Belov, and Y. S. Kivshar, *Opt. Exp.*, **20**, 20599–20604 (2012).
27. S. V. Gaponenko, P. M. Adam, D. V. Guzatov, and A. O. Muravitskaya, *Sci. Rep.*, **9**, 7138–7146 (2019).
28. D. V. Guzatov, *Effect of Nanoobjects of Complicated Configuration on the Characteristics of Spontaneous Emission of Atoms and Molecules*, Doctoral Dissertation in Physical-Mathematical Sciences, Grodno (2019).
29. D. V. Guzatov, S. V. Vaschenko, V. V. Stankevich, A. Ya. Lunevich, Y. F. Glukhov, and S. V. Gaponenko, *J. Phys. Chem. C*, **116**, 10723–10733 (2012).
30. S. V. Gaponenko and D. V. Guzatov, *Chem. Phys. Lett.*, **477**, 411–414 (2009).

31. E. V. Klyachkovskaya, D. V. Guzatov, N. D. Strekal, S. V. Vaschenko, A. N. Harbachova, M. V. Belkov, and S. V. Gaponenko, *J. Raman Spectrosc.*, **43**, 741–744 (2012).
32. A. Rumyantseva, S. Kostcheev, P. M. Adam, S. V. Gaponenko, S. V. Vaschenko, O. S. Kulakovich, A. A. Ramanenka, D. V. Guzatov, D. Korbutyak, V. Dzhagan, and A. Stroyuk, *ACS Nano*, **7**, 3420–3426 (2013).
33. V. V. Klimov, *Nanoplasmonics* [in Russian], Fiz.-Mat. Lit., Moscow (2009).
34. S. V. Gaponenko, D. V. Guzatov, and N. D. Strekal, *J. Phys. Chem. C*, **125**, 27654–27660 (2021).
35. Y. C. Chen and G. Bahl, *Optica*, **2**, 893–899 (2015).
36. Yu. I. Grenberg (ed.), *Technology, Study, and Storage of Easel and Wall Paintings* [in Russian], Izobrazitel′noe Iskusstvo, Moscow (1987).
37. J. M. Madariaga, *Anal. Methods*, **7**, 4848–4876 (2015).
38. P. Vandenabeele, H. G. Edwards, and L. Moens, *Chem. Rev.*, **107**, 675–686 (2007).
39. K. Chen, K.-C. Vo-Dinh, F. Yan, M. B. Wabuyele, and T. Vo-Dinh, *Anal. Chim. Acta*, **569**, 234–237 (2006).
40. K. L. Wustholz, C. L. Brosseau, F. Casadio, and R. P. Van Duyne, *Phys. Chem. Chem. Phys.*, **11**, 7350–7359 (2009).
41. C. L. Brosseau, K. S. Rayner, F. Casadio, C. M. Grzywacz, and R. P. Van Duyne, *Anal. Chem.*, **81**, 7443–7447 (2009).
42. A. G. Milekhin, L. L. Sveshnikova, T. A. Duda, N. V. Surovtsev, S. V. Adichtchev, Yu. M. Azhniuk, C. Himcinschi, M. Kehr, and D. R. T. Zahn, *J. Phys.: Conf. Ser.*, **245**, Article ID 012045 (2010).
43. J. T. Hugall, J. J. Baumberg, and S. Mahajan, *Appl. Phys. Lett.*, **95**, Article ID 141111 (2009).
44. M. V. Chursanova, V. M. Dzhagan, V. O. Yukhymchuk, O. S. Lytvyn, M. Ya. Valakh, I. A. Khodasevich, D. Lehmann, D. R. T. Zahn, C. Waurisch, and S. G. Hickey, *Nanoscale Res. Lett.*, **5**, 403–409 (2010).
45. A. Rumyantseva, S. Kostcheev, P. M. Adam, S. V. Gaponenko, S. V. Vaschenko, O. S. Kulakovich, A. A. Ramanenka, D. V. Guzatov, D. Korbutyak, V. Dzhagan, and A. Stroyuk, *ACS Nano*, **7**, 3420–3426 (2013).
46. E. Klyachkovskaya, N. Strekal, I. Motevich, S. Vaschenko, A. Harbachova, M. Belkov, S. Gaponenko, Ch. Dais, H. Sigg, T. Stoica, and D. Grutzmacher, *Plasmonics*, **6**, 413–418 (2011).
47. E. V. Klyachkovskaya, N. D. Strekal, I. G. Motevich, S. V. Vashchenko, M. Ya. Valakh, A. N. Gorbacheva, M. V. Belkov, and S. V. Gaponenko, *Opt. Spectrosc.*, **110**, 48–54 (2011).
48. E. V. Shabunya-Klyachkovskaya, S. V. Gaponenko, S. V. Vaschenko, V. V. Stankevich, N. P. Stepina, and A. S. Matsukovich, *J. Appl. Spectrosc.*, **81**, 399–403 (2014).
49. E. Shabunya-Klyachkovskaya, O. Kulakovich, S. Vaschenko, D. Guzatov, and S. Gaponenko, *Eur. J. Sci. Theol.*, **12**, No. 3, 211–220 (2016).
50. E. V. Shabunya-Klyachkovskaya, E. V. Korza, L. L. Trotsyuk, A. S. Matsukovich, and O. S. Kulakovich, *Opt. Spektrosk.*, **122**, No. 1, 66–70 (2017).
51. E. V. Shabunya-Klyachkovskaya, O. S. Kulakovich, and S. V. Gaponenko, *Spectrochim. Acta, Part A*, **222**, Article ID 117235 (2019).
52. O. Kulakovich, E. Shabunya-Klyachkovskaya, L. Trotsiuk, A. Matsukovich, and Y. Korza, *J. Raman Spectrosc.*, **50**, No. 7, 936–944 (2019).
53. O. S. Kulakovich, E. V. Shabunya-Klyachkovskaya, A. S. Matsukovich, L. L. Trotsiuk, and S. V. Gaponenko, *J. Appl. Spectrosc.*, **83**, 860–863 (2016).
54. E. V. Shabunya-Klyachkovskaya, O. S. Kulakovich, A. G. Mitskevich, Y. F. Moiseev, V. V. Kiris, A. S. Matsukovich, A. G. Karoza, L. L. Sysoeva, and M. V. Belkov, *J. Cult. Heritage*, **28**, 158–163 (2017).
55. E. V. Klyachkovskaya, N. M. Kozhukh, V. A. Rozantsev, and S. V. Gaponenko, *J. Appl. Spectrosc.*, **72**, 371–375 (2005).
56. E. V. Shabunya-Klyachkovskaya, V. V. Kiris, A. N. Shimko, M. V. Belkov, and S. N. Raikov, *J. Appl. Spectrosc.*, **80**, 922–929 (2014).